Structure, reactivity, and electronic properties of V-doped Co clusters

Soumendu Datta,[1] Mukul Kabir,[2] Tanusri Saha-Dasgupta,[1] and Abhijit Mookerjee[1]
[1]*Department of Material Sciences, S. N. Bose National Centre for Basic Sciences, JD Block, Sector-III, Salt Lake City, Kolkata 700 098, India*
[2]*Department of Materials Science and Engineering, Massachusetts Institute of Technology, Cambridge, Massachusetts 02139, USA*
(Received 19 April 2009; revised manuscript received 8 July 2009; published 14 August 2009)

Structures and physicochemical properties of V-doped Co_{13} clusters have been studied in detail using density-functional-theory-based first-principles method. We have found anomalous variation in stability of the doped clusters with increasing V concentration, which has been nicely demonstrated in terms of energetics and electronic properties of the clusters. Our study explains the nonmonotonic variation in reactivity of $Co_{13-m}V_m$ clusters toward H_2 molecules as reported experimentally [Nonose *et al.*, J. Phys. Chem. **94**, 2744 (1990)]. Moreover, it provides useful insight into the cluster geometry and chemically active sites on the cluster surface, which can help to design better catalytic processes.

DOI: 10.1103/PhysRevB.80.085418 PACS number(s): 73.22.−f, 36.40.Cg

I. INTRODUCTION

The interest in the studies of clusters is largely because of their possible technological applications which include the possibilities of developing novel cluster-based materials using the size dependence of their properties. Doping of clusters is an important possibility in this direction. In recent times, the fabrication of alloy clusters of different sizes with well defined, controlled properties by varying the composition and atomic ordering has caught considerable attention.[1,2] Bimetallic alloy clusters have been known and exploited for last few years in various applications, especially in the catalytic reactions.[3,4] Varying the ratio of the two constituents, one can alter the surface structures, compositions, and segregation properties.[5,6] In this way, it is possible to tune the chemical reactivity at the surface of an alloyed cluster.[7,8] Considering the huge possibility of using nanoclusters in catalysis, the study of cluster reactivity has become an interdisciplinary topic of present day research.[9–12]

About 2 decades ago, Nonose *et al.* measured the reactivity toward H_2 of bimetallic Co_nV_m $(n>m)$ clusters using laser-vaporization technique and reported strong cluster size and composition dependence.[13] Both V and Co are 3*d* transition metals. The substitution of Co by V atoms, one by one, should increase the reactivity of the alloy cluster toward H_2 molecules as V, an early transition metal, has a high reactivity toward H_2 in contrast to Co which has relatively low reactivity.[14] Interestingly, it was found that the reactivity increased gradually, as expected, with the substitution of Co atom by V atom one by one in the Co_n clusters $(n<13)$, but for the Co_{13}, there was a remarkable decrease in reactivity when a single Co atom was substituted by a V atom. However, the reactivity increased as the number of exchange V atoms increased further up to $m=3$, while the fourth V-atom substitution did not increase the reactivity any more. In view of the high reactivity of elemental V, this sudden drop in reactivity of the $Co_{12}V$ cluster was rather surprising. The authors speculated a plausible icosahedral structure for the $Co_{12}V$ cluster with the active V atom at the cage center. Therefore, the V atom, being shielded geometrically from H_2 by the 12 surface Co atoms, might have less chance to interact with H atoms. The chemisorption reactivity of cationic $Co_{13-m}V_m^+$ clusters[15] and anionic $Co_{13-m}V_m^-$ clusters[16] also shows similar type of variation as that of neutral $Co_{13-m}V_m$ clusters, which hints toward the dominant effect of geometric structure as compared to the electronic structure. For clusters, the ionization potential (IP) depends on the position of the highest occupied molecular-orbital (HOMO) level. For the pure metal clusters, Whetten *et al.* postulated that the reaction rate for cluster-H_2 dissociative chemisorption is determined by the charge transfer from the HOMO to the lowest unoccupied molecular-orbital (LUMO) of the reactant gas H_2 and an anticorrelation between IP and reaction coefficient could be observed.[17] That means lower value of IP corresponds to higher reactivity and vice versa. However, the ionization energies of the Co_nV_m clusters, measured by Hoshino *et al.* using photoionization spectroscopy show no such anticorrelation,[18] again demonstrating the importance of geometrical structure. A rigorous first-principles study in terms of geometric and electronic effects is therefore very much needed to understand this anomalous nature of reactivity of $Co_{13-m}V_m$ $(m=0-4)$ clusters. In this paper, we have carried out an *ab initio* theoretical study on V-doped Co_{13} clusters. The whole study can be divided into three major parts. First part consists of an exhaustive search for the minimum-energy structures (MESs) for cluster of each composition, followed by stability analysis of these MESs in terms of various physical quantities in the second part, while the final part includes investigation of chemisorbed structures and understanding of cluster reactivity.

II. COMPUTATIONAL DETAILS

The calculations have been performed using density-functional theory (DFT), within the pseudopotential plane-wave method as implemented in VASP code.[19] We have used the projector augmented wave (PAW) pseudopotentials[20,21] and the Perdew-Burke-Ernzerhof (PBE) exchange-correlation functional[22] for spin-polarized generalized gradient approximation (GGA). The 3*d* and 4*s* electrons were treated as the valence electrons for the transition-metal elements and the wave functions were expanded in the plane-wave basis

set with the kinetic-energy cutoff of 335 eV. The convergence of the cluster energies with respect to the cutoff value has been checked. Reciprocal space integrations were carried out at the Γ point. Symmetry unrestricted geometry and spin optimizations were performed using the conjugate gradient and the quasi-Newtonian methods until all the force components were less than a threshold value of 0.005 eV/Å. In order to ensure the structural trends found in the optimized structures, we have also carried out Bohn-Oppenheimer molecular dynamics[23] within local-density approximation (LDA) for few specific clusters. Simple cubic supercells were used for cluster calculations with the periodic boundary conditions, where two neighboring clusters were kept separated by at least 12 Å vacuum space to make the interaction between the cluster images negligible. The cohesive energy (E_c) of a Co_nV_m alloy cluster is calculated with respect to the free atoms as

$$E_c(Co_nV_m) = mE(V) + nE(Co) - E(Co_nV_m), \quad (1)$$

where $E(Co_nV_m)$, $E(Co)$, and $E(V)$ are the total energies of Co_nV_m cluster, an isolated Co atom, and an isolated V atom, respectively. One can also define the cohesive energy with respect to the Co and V bulk phases at equilibrium instead of isolated atoms. However, the cohesive energy variation with increasing V concentration follows the same trend irrespective of the way of cohesive energy definition. The second difference in energy for fixed size ($n+m$=constant) and variable composition is defined as

$$\Delta_2 E(Co_nV_m) = E(Co_{n+1}V_{m-1}) + E(Co_{n-1}V_{m+1}) - 2E(Co_nV_m). \quad (2)$$

It gives the relative stability of alloy clusters having nearby compositions.

III. STRUCTURE

Since chemical reaction with clusters takes place on its surface, the atomic arrangement and the composition of cluster surface play an important role in chemical reactivity. Therefore, the first step toward the theoretical modeling of clusters is to determine their ground-state structure. In our earlier work,[24] we studied the structure and magnetism of the pure Co clusters in detail. To obtain the MES having the optimized geometry as well as the optimized magnetic moment, we considered several probable starting geometries having closed packed atomic arrangement and allowed each of the geometries to relax for *all possible* collinear spin configurations of the atoms. We follow the same way of structural optimization here for the V-doped Co clusters ($Co_{13-m}V_m$; m=1–4). However, the situation for alloy clusters is quite cumbersome as one has to deal with a large number of starting geometries because of the presence of *homotops* (the term was first coined by Jellinek[25,26]). The *homotops* have the same number of atoms, composition, and geometrical structure, but differ in the arrangement of the doped atoms. As for example, a single geometrical structure of an A_nB_m alloy cluster with fixed number of atoms ($N=m+n$) and composition (m/n ratio) will give, in principle, $\frac{N!}{m!n!}$ *homotops*. Some of them, however, may be symmetry equivalent and the number of the inequivalent *homotops* will be somewhat less than the above-mentioned value. So the variety of structures in alloy clusters is much richer than that of the pure clusters and the potential-energy surface of even a small cluster of few tens of atoms is of enormous complexity.

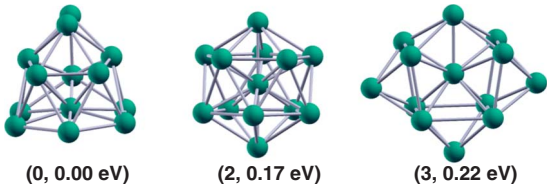

FIG. 1. (Color online) Structures of optimal HCP, icosahedron, and cuboctahedron of pure Co_{13} cluster (from left to right, respectively). The first entry in the parenthesis gives the isomeric position ("0" means minimum-energy state) and the second entry corresponds to relative energy to the minimum-energy state.

It is generally found that the transition-metal clusters prefer compact geometries to maximize the interaction between the rather localized *d* orbitals.[27] There are three most compact and highly coordinated structures for 13 atoms cluster: icosahedron, cuboctahedron, and hexagonal closed packed (HCP) geometries. We have therefore considered these three geometries as the most probable starting structures. For the pure Co_{13} cluster, we found that the MES is a distorted HCP geometry with total magnetic moment of $25\mu_B$ and total cohesive energy of 42.63 eV as mentioned in our previous work.[24] The structure has 22 triangular faces and 33 edges (cf. Fig. 1). This hexagonal growth of the pure Co clusters is quite unusual compared to the trend seen in the clusters of its 3*d* neighbors such as Mn, Fe, and Ni, which preferably adapt an icosahedral pattern.[28–30] Further study is needed to explore the unusual structural pattern of small pure Co clusters.[31,32] Another distorted structure of HCP motif with total magnetic moment of $27\mu_B$ and 0.14 eV above the minimum-energy state is the first isomer. The optimal icosahedral structure of total spin $31\mu_B$ (structure having 20 triangular faces and 30 edges) is 0.17 eV higher than the minimum-energy state and emerges as the second isomer. The third isomer is a distorted cuboctahedron with total magnetic moment $25\mu_B$ and it is 0.22 eV above the minimum-energy state. The structures of the ground state, second and third isomers are shown in Fig. 1. It is to be noted that for the pure Co_{13} cluster, all the atomic moments are ferromagnetically coupled and our predicted magnetic moment of the ground-state structure is in good agreement with the experimental value which is $2.0\mu_B$/atom.[33]

In the case of single V atom doped $Co_{12}V$ clusters, we have again considered the starting geometries of icosahedral, HCP, and cuboctahedral symmetries. However, depending upon the position of the singly doped V atom either at the center or on the surface, it can give rise to several *homotops*. Again, the surface atoms of a 13-atom cluster are not equivalent in terms of number of neighbors and their relative positions in case of HCP and cuboctahedral structures, while for icosahedral structure, all the surface atoms are equivalent. This consideration will give few more starting geometries.

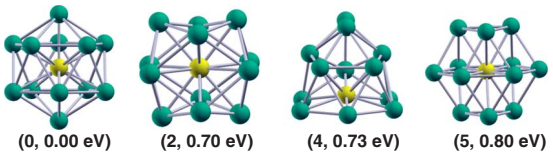

FIG. 2. (Color online) Structures of optimal icosahedron, optimal cuboctahedron, and two HCP geometries (from left to right) for $Co_{12}V$ cluster. Green (black) dot represents Co atom, while yellow (gray) dot represents V atom. The entries in the parentheses have the same meaning as in Fig. 1.

So we have considered all these possible geometrical structures and for each of them, we have considered the *all possible* collinear spin alignments during relaxation. Upon optimization of geometry and spin degrees of freedom, we find that an icosahedral structure of total magnetic moment $25\mu_B$, with V atom doped at the center position, is the MES. Now there are several interesting points to note in the context of the $Co_{12}V$ cluster. First of all, the cohesive energy of the MES is considerably higher (by 1.29 eV) than that of the pure Co_{13} clusters, indicating its exceptional stability. Second, the V-doped Co clusters are found to prefer the icosahedral growth pattern, instead of HCP growth pattern, as we observed in case of the pure Co clusters. Therefore, just the single V-atom doping in Co_{13} changes the equilibrium structure from HCP to icosahedron. This HCP to icosahedron structural transition has also been reported previously for Mn doping in Co_{13} cluster.[34] Finally, the single V atom likes to fit at the center of the icosahedron and it is ferrimagnetically coupled with the surface Co atoms. The first isomer is also a central V-atom-doped icosahedral $Co_{12}V$ cluster, with total magnetic moment $23\mu_B$ and it is about 0.46 eV above the MES. Center V-doped cuboctahedral $Co_{12}V$ cluster with $23\mu_B$ magnetic moment which has energy 0.70 eV higher than the minimum-energy icosahedral structure is the second isomer. The third isomer is a center V-doped icosahedron with total magnetic moment of $27\mu_B$. Center V doping in case of HCP cluster is less favorable and appears as the fifth isomer in our calculation with total magnetic moment $25\mu_B$ and energy 0.80 eV above the MES. We have also considered the optimal structure of Co_{13} (distorted HCP) as the starting structure and substituted the most coordinated central Co atom by a V atom. After relaxation, considering *all possible* spin alignments, it is found that the shape of the optimal structure remains more or less same as that of the optimal HCP Co_{13} cluster and energetically, it is the fourth isomer with total magnetic moment $23\mu_B$. The most probable surface V doping has a cuboctahedral structure with total magnetic moment $21\mu_B$, but it is about 1.32 eV above the MES. The structures of ground state and few isomers for the $Co_{12}V$ cluster are shown in Fig. 2.

Because of the icosahedral growth preference of the $Co_{12}V$ cluster and the presence of the singly doped V atom at the central site, we consider only the icosahedral-symmetry-based geometries as the starting guess for more than one V-atom-doped clusters, in which one V atom is always at the center position, while the residual V atoms reside on the surface. For $Co_{11}V_2$ cluster, the second V atom can replace any of the surface Co atoms, as all the surface sites of a 13-atom icosahedron are equivalent. After relaxation for *all possible* spin configurations, we find that the MES has total magnetic moment of $19\mu_B$ and total cohesive energy of 43.22 eV. The first and second isomers have magnetic moments of $21\mu_B$ and $17\mu_B$ and they are 0.10 and 0.25 eV above the minimum-energy state, respectively. In the MES, the center V atom is again ferrimagnetically coupled with the surface Co atoms and has much lower local magnetic moment as it was in the case of the $Co_{12}V$ cluster, while the surface V atom has the maximum local magnetic moment and it is also ferrimagnetically coupled with the other surface Co atoms.

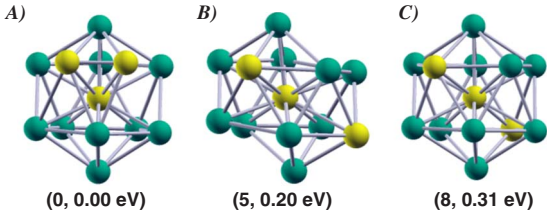

FIG. 3. (Color online) *A*, *B*, and *C* represent the three inequivalent homotops in icosahedral $Co_{10}V_3$ structure having one V atom always at the center. The three structures are the optimal structures for the respective three types. The entries in the parentheses have the same meaning as in Fig. 1. Color convention for atoms is the same as in Fig. 2.

For $Co_{10}V_3$ cluster, depending on the different positions of the two surface V atoms, there are three possible icosahedral structures as shown in Fig. 3. However, the structure of type *A* where the two surface V atoms are closest to each other appears as the most favorable one. This type *A* icosahedral structure with total magnetic moment of $21\mu_B$ is the minimum-energy state with ferrimagnetic alignment of the central V atom and ferromagnetic alignment of the surface V atoms with the surface Co atoms. Both the central and the surface V atoms have small values of local magnetic moments in this case. There are several closely spaced isomers of type-*A* icosahedron with magnetic moments of $19\mu_B$, $13\mu_B$, $23\mu_B$, and $17\mu_B$ which are just 0.04, 0.08, 0.09, and 0.15 eV above the MES. We find that the optimal structures of type *B* and type *C* are 0.20 and 0.31 eV above the MES, respectively, and both of them have same total magnetic moment of $13\mu_B$.

For Co_9V_4, there are three V atoms on the surface. Considering two surface V atoms at closest to each other (following the ground-state configuration of $Co_{10}V_3$), different positions of the third surface V atom can give rise to the four icosahedral configurations as shown in Fig. 4. After optimization, it is found that the type *A* is the most favorable structure where all the three surface V atoms are closest to each other and form an octahedron with the central V atom. The optimal structure of type *A* icosahedron has total magnetic moment of $15\mu_B$ and total cohesive energy of 42.35 eV. Another type-*A* icosahedrons with magnetic moments of $13\mu_B$, $19\mu_B$, $21\mu_B$, and $17\mu_B$ are just 0.03, 0.07, 0.09, and 0.13 eV above the MES. The optimal type-*B*, type-*C*, and type-*D* icosahedrons have total magnetic moments of $15\mu_B$, $13\mu_B$, and $15\mu_B$ respectively, and they are 0.15, 0.25, and 0.33 eV above the MES.

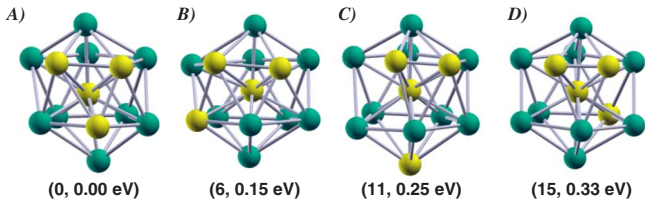

FIG. 4. (Color online) *A*, *B*, *C*, and *D* represent the four probable homotops in icosahedral Co_9V_4 structure having one V atom at the center and two of the remaining three V atoms are closest to each other on the surface, while the position of the fourth V atom is varied. The four structures represented above are the optimal structures for the respective four types. The entries in the parentheses have the same meaning as in Fig. 1. Color convention for atoms is the same as in Fig. 2.

The results of the structural optimizations, therefore, can be summarized as, unlike a HCP growth pattern of the pure Co cluster, the V-doped Co_{13} clusters prefer to adopt an icosahedral packing. In such clusters, the most coordinated central site is occupied by a V atom, while the residual V atoms sit on the surface. The surface V atoms like to be closer to each other to form a group, thereby imparting more distortion to the structure and significantly alter the local surface charge density. The central V site in the MES of all compositions is always ferrimagnetically coupled and has lower magnetic moment. On the other hand, the surface V atoms can be ferrimagnetically or ferromagnetically coupled with the surface Co atoms and their local magnetic moments can be as low as the central V site or as high as the surface Co site, depending on the distribution of surface charge density in the clusters having different amount of V doping. Our prediction of icosahedral geometry for the minimum-energy states of V-doped Co clusters is in accordance with the speculation of a closed-shell geometry around the central site in Refs. 13 and 15.

To have more confidence about the structural trend as observed above, we have carried out few *ab initio* molecular dynamics (MD) study for the $Co_{12}V$ and $Co_{10}V_3$ clusters. To determine the lowest energy structures, we have heated up the clusters to 2000 K (which is close to the melting temperature 1768 K for bulk Co and 2183 K for bulk V). The clusters have then been maintained at this temperature for at least 6 ps and then allowed to cool again to 0 K. The cooling process has been done for 24 ps and maintained a very slow cooling rate of 1 K per one iteration throughout the process. The main results obtained from the MD run are: (a) it prefers to adopt the icosahedral pattern with same magnetic alignment of atoms as we predicted from zero-temperature relaxation; (b) for the $Co_{12}V$ cluster, the V atom occupies the central position; (c) the surface V atoms for the $Co_{10}V_3$ cluster prefer to be closest to each other. These results provide reassurance and more confidence in our zero-temperature relaxation.

IV. STABILITY ANALYSIS

The observed atomic arrangement of the MES of the $Co_{13-m}V_m$ clusters as described in the previous section depends critically on the balance of several parameters like the relative strengths of various kinds of bonds present in a cluster structure, the relative atomic sizes, the amount of charge transfer between two different species of atoms, the energy gap between the HOMO and the LUMO, abundance of states near Fermi energy, etc. Below, we try to understand the structural stability of the clusters in terms of these parameters.

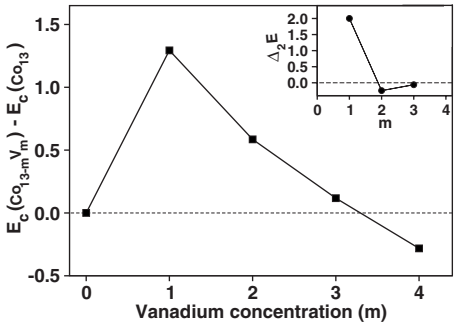

FIG. 5. Cohesive energy of the minimum-energy structures of $Co_{13-m}V_m$ clusters with respect to the cohesive energy of minimum-energy pure Co_{13} cluster. The dashed line is the reference fixed at the cohesive energy of pure Co_{13}. Inset shows the second difference ($\Delta_2 E$) in cohesive energy [as defined in Eq. (2)] for $Co_{12}V$, $Co_{11}V_2$, and $Co_{10}V_3$.

A. Cohesive energy

Figure 5 shows the plot of the cohesive energies of the MES of the $Co_{13-m}V_m$ clusters with increasing V concentration. The plot is with respect to the cohesive energy of the MES of Co_{13} cluster. It is seen that the binding has increased considerably compared to that of the optimal Co_{13} cluster with single V atom doping. However, the cohesive energies decrease sharply for the higher concentration of V atoms. For the double and triple V-atom doping, the cohesive energies are above the dashed line indicating their higher stability compared to the pure Co_{13}, while for the fourth V-atom doping, the cohesive energy is even lower than that of the pure Co_{13}. The relative stability among the clusters of nearby concentrations is more distinct when we plot the second difference in cohesive energies in the inset of Fig. 5. We use Eq. (2) to calculate the second difference. A sharp pick in the $\Delta_2 E$ at $m=1$ points to the exceptional stability of the single V-doped cluster compared to the undoped or more than one V-doped clusters.

In order to understand the stability of the doped clusters, we have calculated the cohesive energies and the bond lengths of the Co-Co, Co-V, and V-V dimers as shown in Table I. It is seen that the V_2 dimer is the most stable and the bond length of the V_2 dimer is also about 14% shorter than that of the Co_2 dimer which has the least binding among the three. On the other hand, the cohesive energy and bond length of the Co-V dimer are intermediate of the Co_2 and the V_2 dimers. For the $Co_{12}V$ cluster, we have seen that the center doping in icosahedral structure is the most favorable. Binary clusters are known to have the problem of segregation, where the doped atom can segregate at the surface or

TABLE I. Cohesive energies and bond lengths of Co_2, Co-V, and V_2 dimers in the present calculation. For comparison, we have also listed the experimental values for Co_2 dimer (Ref. 35) and V_2 dimer (Ref. 36).

	Cohesive energy (eV/atom)		Bond length (Å)	
Dimer	Theory	Expt.	Theory	Expt.
Co_2	1.45	1.72	1.96	2.31
CoV	1.53		1.87	
V_2	1.81	2.47	1.72	1.77

center. To a first approximation, if one of the homonuclear bonds is the strongest, then that species tends to be at the center of the cluster.[1] Our finding of central V doping is in accordance with this, as the V_2 dimer has the strongest binding. The atomic radius of a Co atom and a V atom, being almost same, the substitution of the central Co atom in an icosahedral Co_{13} cluster by a V atom leaves the structure almost unperturbed. As for evidence, the center to vertex average distance and the average distance between two nearby vertices in the optimal icosahedral structure of the Co_{13} cluster are 2.334 and 2.450 Å. For the optimal $Co_{12}V$ cluster, these values are almost same, 2.344 and 2.465 Å, respectively. Therefore, the large gain in cohesive energy of the $Co_{12}V$ cluster over that of the Co_{13} cluster may be due to the enhanced cohesive energy of the CoV dimer over that of the Co_2 dimer, though an atom in a dimer is quite different from an atom at the center of a 13-atom cluster. The V atom being at the central position, there are maximum number of CoV dimers in V-doped clusters.

For the clusters doped with more than one V atom, the favorable structure is again found to be of an icosahedral motif, in which the central site is always possessed by a V atom and the other V atoms lie on the surface. The number of the surface V atoms and the V-V bonds, therefore, increases with increasing V doping. It favors better binding. On the other hand, the presence of the V atoms on the cluster surface distorts the cluster geometry and increases the center to vertex average distance as well as the vertex-vertex average distance. Effectively, the cluster volume increases with the increasing V concentration, which destabilizes the structure. In Table II, we have listed the average distances between center to vertex as well as between two nearby vertices for the MES of $Co_{13-m}V_m$ (m=0–4). We believe that the distortion in the structures is due to the charge-density variation induced by the presence of the V atoms on the cluster surface. The strained cluster structures resulted from distortion can be realized from some open bonds in Figs. 3 and 4. Therefore, though the number of the V-V bonds increases, which has better binding compared to the Co-Co or Co-V bonds, the overall cohesive energy decreases monotonically as we go from $Co_{12}V$ to Co_9V_4 by successive doping of V atoms. It is then obvious that the cluster geometry and the distribution of atoms on the cluster surface play an important role in deciding the cluster stability.

At this point, it is interesting to study the structure and energetics of the pure V_{13} cluster. Since experiment hints symmetric structure for the V_{13} cluster,[37] we considered an icosahedral geometry and optimized it considering *all possible* spin configurations. Interestingly, the decreasing trend of cohesive energies for the $Co_{13-m}V_m$ clusters with increasing V concentration continues also at m=13, i.e., pure V_{13} cluster. The cohesive energy of the optimal V_{13} cluster is found to be lower than that of the pure Co_{13} cluster by about 3.73 eV. It indicates that V_{13} would be more reactive than any of the V-doped Co_{13} clusters. This tendency may be rationalized by considering the case of bulk V and Co, where the bulk V is more reactive than Co because of the lower *d*-band filling, relatively higher position of *d*-band center, and larger *d*-band width of V compared to Co. However, pure V does not have importance in catalysis because its high reaction tendency with absorbate tends to poison the surface without leaving any active site. The desorption energy is also high because of strong V-absorbate bond, which is again not favorable for catalysis.

B. Spin gap

Analogous to HOMO-LUMO gap of a nonmagnetic cluster, one can define spin gaps for a magnetic cluster as,

$$\delta_1 = -[\epsilon_{\mathrm{HOMO}}^{\mathrm{majority}} - \epsilon_{\mathrm{LUMO}}^{\mathrm{minority}}],$$

$$\delta_2 = -[\epsilon_{\mathrm{HOMO}}^{\mathrm{minority}} - \epsilon_{\mathrm{LUMO}}^{\mathrm{majority}}], \quad (3)$$

and the system is said to be stable if both δ_1 and δ_2 are positive, i.e., the LUMO of the majority spin lies above the HOMO of the minority spin and vice versa. These represent the energy required to move an infinitesimal amount of charge from the HOMO of one spin channel to the LUMO of the other. So magnitude of spin gaps is a measure of chemical activeness of clusters. Higher gap means less reactive and vice versa. The positions of the HOMO and LUMO in both the spin channels and the values of δ_1 and δ_2 for the optimized structures of 13-atom V-doped Co clusters of all compositions considered here are given in Table III. It is seen that both the spin gaps δ_1 and δ_2 are positive for all the clusters. Also, $Co_{12}V$ has the maximum value of δ's which

TABLE II. The average distances in Å between center to vertex and between two nearby vertices for the minimum-energy structures of all the studied clusters. For Co_{13}, the values correspond to the optimal icosahedron.

Bonds	Co_{13}	$Co_{12}V$	$Co_{11}V_2$	$Co_{10}V_3$	Co_9V_4
Center-vertex	2.334	2.344	2.354	2.375	2.398
Vertex-vertex	2.455	2.465	2.476	2.499	2.509

TABLE III. Positions of HOMO and LUMO in both the spin channels and the values of δ_1 and δ_2 for the optimized structures of all compositions.

	Majority channel		Minority channel		Spin gap (eV)	
Cluster	HOMO	LUMO	HOMO	LUMO	δ_1	δ_2
Co_{13}	−3.60	−3.35	−3.48	−3.34	0.26	0.13
$Co_{12}V$	−3.93	−2.61	−3.39	−3.34	0.59	0.78
$Co_{11}V_2$	−3.71	−2.83	−3.43	−3.32	0.39	0.60
$Co_{10}V_3$	−3.41	−2.98	−3.34	−3.26	0.15	0.36
Co_9V_4	−3.46	−3.02	−3.33	−3.17	0.29	0.31

again indicates the highest stability of $Co_{12}V$ cluster compared to the others. Because of this large spin gap, $Co_{12}V$ has very low reaction tendency toward H_2 molecules. However, gap values decrease with increasing V concentration and therefore reactivity also increases as observed experimentally.[13]

C. Density of states

Figure 6 shows the spin-polarized total density of states (DOS), Co-projected DOS, V-projected DOS, and total *d*-orbital-projected DOS for the MES of $Co_{12}V$, $Co_{11}V_2$, $Co_{10}V_3$, and Co_9V_4 clusters. It is seen that the total DOS and the total *d*-projected DOS are almost overlapping each other. This indicates that the cluster properties are mostly dominated by the *d*-electrons which is generally expected for transition-metal clusters. The trend in structural stability and reactivity of the clusters as discussed in the previous sections is also obvious from the nature of the total DOS. The majority-spin channel of each cluster has a gap. This gap is maximum for the $Co_{12}V$ cluster and it decreases as the number of surface V atoms increases. In the minority-spin channel, there is finite amount of states at the Fermi energy and these are contributed solely by the exterior surface atoms, as the central atom does not have any contribution at the Fermi energy (cf. Fig. 7). It is also seen that the states are more localized in case of the $Co_{12}V$ cluster, while they are gradually spreading out and therefore the DOS height, especially in the majority-spin channel, decreases with the increasing V concentration. At this point, it is relevant to mention a com-

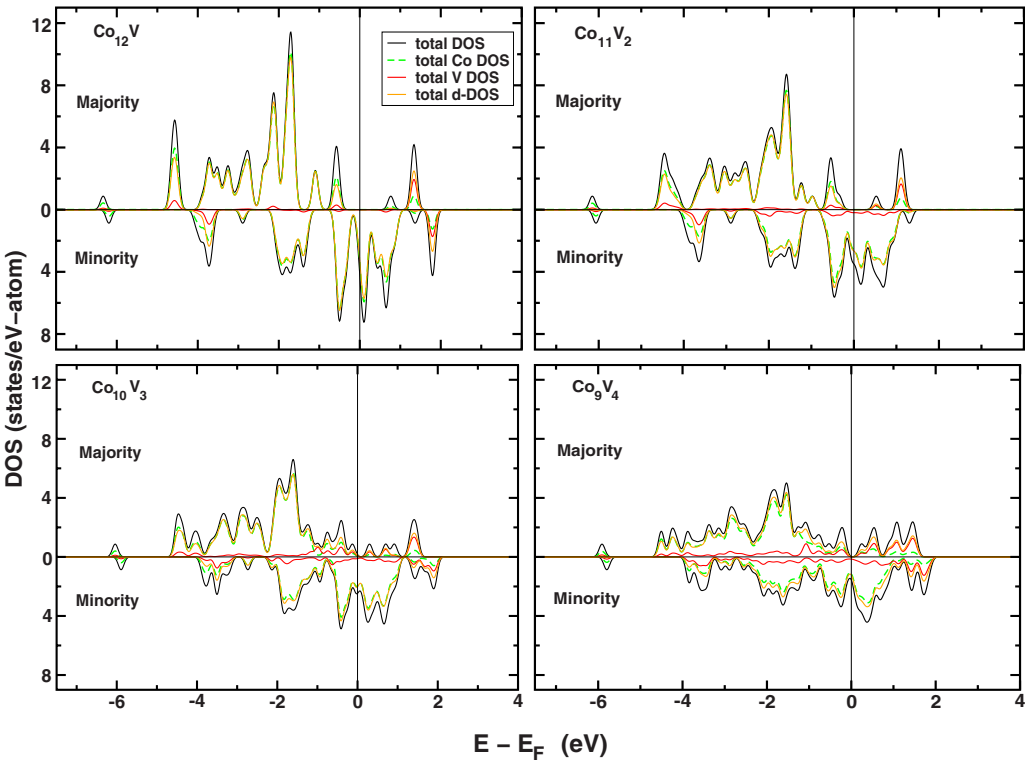

FIG. 6. (Color online) Total DOS per atom, Co projected DOS per atom, V-projected DOS per atom, and total *d*-projected DOS per atom for the optimal structures of $Co_{12}V$, $Co_{11}V_2$, $Co_{10}V_3$, and Co_9V_4. The smearing width is fixed at 0.1 eV. Vertical line through zero is the Fermi energy (E_F).

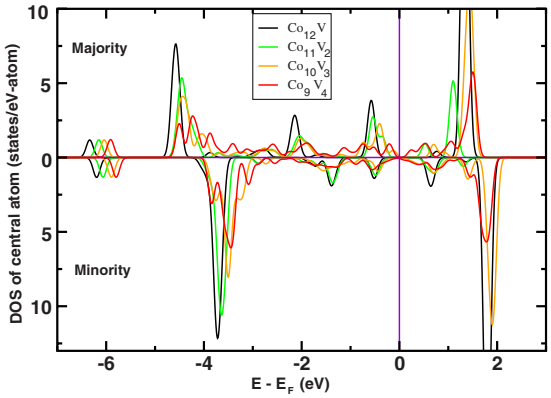

FIG. 7. (Color online) Total DOS of the central V atom in the optimal structures of $Co_{12}V$, $Co_{11}V_2$, $Co_{10}V_3$, and Co_9V_4. The Fermi energy (E_F) is fixed at zero.

mon feature observed in case of extended surface. The gaseous molecules absorb well on clean surface of an early transition metal as well as on the surface with a multilayer of late transition metal, but not on the surface with a monolayer of late transition metal. For example, the photoemission experiments by El-Batanouny *et al.*[38] showed that a *H* atom adsorbs well both on the clean Nb(110) surface as well as on the surface with a multilayer of Pd, but does not adsorb on Nb(110) surface with a monolayer of Pd and this is due to the decrease of density of states of *d* electrons of Pd near the Fermi level. Similar behavior had been observed also in case of a monolayer of Pd on W(110) surface in the experiment of CO adsorption.[39] Although, a cluster of 13 atoms is substantially different in its property from that of the surface or bulk, one may resemble the stability of the $Co_{12}V$ cluster toward H adsorption with that of extended surface, where the central V atom of $Co_{12}V$ corresponds to an early transition-metal substrate and the exterior 12 Co atoms correspond to a late transition-metal monolayer.

In order to see the chemical activity of the central V atom, we have plotted in Fig. 7 the projected total DOS of the central V atom for each of the $Co_{13-m}V_m$ clusters. First of all, it is seen that there is no finite states at the Fermi energy, meaning that the central V atom is not chemically active. Also, each of the majority- and minority-spin channels has two large pecks: one is deep below the Fermi energy and another is above the Fermi energy. However, the peck heights gradually decrease; the states are broadened out and shifted toward higher energy with increasing V concentrations. It is therefore indicating that the presence of surface V atoms induces some sort of chemical activeness to the central atom.

V. CHEMISORPTION WITH H_2 MOLECULES

In order to gain some understanding about the cluster chemical reactivity, we have investigated the chemisorbed structures of the $Co_{13-m}V_m$ clusters upon H_2 adsorption. To check the robustness of our chemisorption calculations involving H atoms, we have first calculated the cohesive energy, bond length, and vibrational frequency of H_2 dimer.

TABLE IV. Theoretical values of cohesive energy, bond length, and vibrational frequency for H_2 dimer in the present calculation. Experimental values in Ref. 41 are also given for comparison.

	Cohesive energy (eV)	Bond length (Å)	Vibrational frequency (cm^{-1})
Theory	4.520	0.752	4339
Experiment	4.750	0.741	4395

Our calculated values have been listed in Table IV. These values are typical for gradient-corrected calculations of H_2, which have been done before[40] and they agreed reasonably well with experiment.[41]

We have then performed an exhaustive search for the MES, taking H_2 at different possible places on the MES of the corresponding bare cluster for each composition. Figure 8 shows our calculated lowest-energy chemisorption structures after H_2 absorption for clusters of all compositions. First thing to notice is that H_2 molecule chemisorbs dissociatively in each case, i.e., the distance between the two H atoms in the chemisorption structures is much larger than the H-H bond length of an isolated H_2 molecule. The chemisorption gives rise to moderate perturbation to the structures and makes them more symmetric (i.e., surface bonds are now less dispersive) compared to the parent structure without hydrogen. There are three possible ways for the H atoms to be adsorbed on each cluster: on top of an atom (one fold), at a bridge position between two atoms (twofold), and at the hollow site of a triangular plane on the cluster (threefold). Again, as the surface contains two species of atoms for $Co_{11}V_2$, $Co_{10}V_3$, and Co_9V_4, then the onefold position can be on top of a surface V atom or on top of a surface Co atom. Twofold position can be the top of a V-V bond, Co-V bond, or a Co-Co bond which can be nearer to or away from the V site. Similarly, in triangular plane, there are several possibilities: (i) all three atoms can be V atoms (only possible for Co_9V_4), (ii) one Co atom and two V atoms, (iii) two Co atoms and one V atom, and (iv) all three are Co atoms. We have considered all these possible combinations during optimization. It is, however, seen that in each of the optimized structures, H atoms absorb at the hollow site on the surface and for $m \geq 2$, they prefer the association of the local V atom. For example, in the $Co_9V_4H_2$ cluster, one H atom absorbs at the hollow site of V-V-V triangular plane and the other H atom on top of a V-V-Co triangular plane. For $Co_{11}V_2H_2$, the H atoms appear to absorb at the bridge posi-

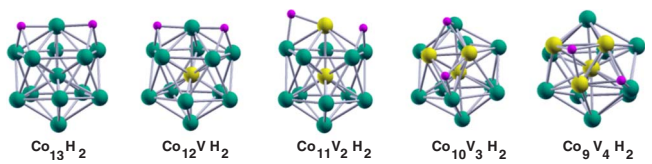

FIG. 8. (Color online) The calculated minimum-energy chemisorption structures with H_2 on the minimum-energy structures of $Co_{13-m}V_m$ (m=0–4). It is clearly seen that hollow site on the surface is preferred by chemisorbed hydrogen. Color convention is the same as in Fig. 2 with small pink colored dots representing H atom.

tions, but they are inclined with an angle such that the absorption tends toward a threefold configuration. The preference of more coordinated hollow site is likely due to geometric arrangements. It allows the H atom to interact more with the V or Co atoms. On the other hand, the V-site preference of H atom is due to the formation of stronger *s*-*d* bond with V atom compared to that with Co atom.

The higher reactivity of the Co_{13} cluster compared to the $Co_{12}V$ cluster, while both of them have the same 12 Co atoms on the surface, can be understood from charge-transfer analysis. We have computed the charge enclosed within a sphere around each surface atom of the optimal structures of $Co_{13}H_2$ and $Co_{12}VH_2$ clusters. It is seen that the amount of charge on the surface Co atoms in the $Co_{13}H_2$ cluster is larger by about 0.2 (in unit of electronic charge) than that of $Co_{12}VH_2$ and it is mainly contributed by the *d* electrons of surface Co atoms. Therefore, stronger 3*d*-1*s* interaction between surface Co atoms and chemisorbed H atoms in case of $Co_{13}H_2$ increases its reactivity. This result is in accordance with that of Fujima and Yamaguchi[42] who also predicted the stronger interaction between 1*s* of H atom and the 3*d* orbital of the surface Co atom in the $Co_{13}H_2$ cluster compared to that in the $Co_{12}VH_2$ cluster using density of state analysis. They showed that the antibonding orbital component between the H 1*s* electron and the 3*d* electron of the surface Co atoms shifts further away above the HOMO in case of $Co_{13}H_2$ compared to that of $Co_{12}VH_2$, while the bonding orbital components for both the clusters stay almost at the same energy position below the HOMO. Extending the charge-transfer analysis for the $Co_{13-m}V_mH_2$ clusters with $m=2$, 3, and 4, we find that the average charge per surface V atom is gradually increasing with the increase of V concentration which indicates the formation of stronger V-H bonds at the surface with increasing V doping. Average charge per surface Co atom for these three clusters, however, remains almost the same.

Figure 9 shows the plot of chemisorption energy with increasing V concentration, where the chemisorption energy is defined as

$$D_e(E) = E(Co_{13-m}V_m) + E(H_2) - E(Co_{13-m}V_mH_2). \quad (4)$$

It is a positive quantity and gives a measure of binding strength of H_2 molecule with the cluster. The plot shows a minimum for $Co_{12}VH_2$, again indicating the lowest binding efficiency of $Co_{12}V$ with H. However, chemisorption energy increases with increasing V concentration. The source of this chemisorption energy is the cluster rearrangement energy (i.e., the energy change due to the geometrical rearrangement of the cluster upon chemisorption) and the efficient cluster-absorbate bonding in presence of V due to more efficient *s*-*d* hybridization.

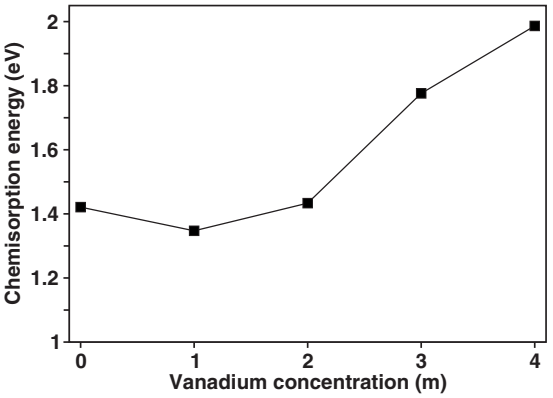

FIG. 9. The calculated chemisorption energy [using Eq. (4)] for $Co_{13-m}V_mH_2$ clusters.

VI. SUMMARY AND CONCLUSIONS

To summarize, we have studied the geometric and electronic structures of V-doped Co_{13} clusters and their chemisorption toward hydrogen molecules using first-principles density-functional calculation. The lowest-energy structures of all compositions prefer to have icosahedral geometry, unlike hexagonal symmetry preference of the pure Co clusters. For the $Co_{12}V$ cluster, the single V atom prefers to sit at the central site, thereby guarded by all the surface Co atoms and cannot participate directly in the chemisorption reaction. Consequently reactivity of $Co_{12}V$ becomes very less. On the other hand, for more than one V atom doping, the additional V atoms reside on the surface and come in direct contact with chemisorbed H atom and reactivity increases. Our calculated spin gaps, density of states, and charge-transfer analysis explain nicely the stability of clusters and their tendency toward chemisorption. In the chemisorbed structures, H atoms adsorb dissociatively at the more coordinated hollow sites and they prefer V site association due to stronger 3*d*-1*s* hybridization. To have better insight into the chemisorption reaction, one needs to study the transition states for the optimal cluster of each composition and we believe that calculation of activation barriers will also lead to same conclusion as we have predicted here.

ACKNOWLEDGMENTS

S.D. is thankful to the Council of Scientific and Industrial Research (Government of India) for financial support. T.S.D. thanks the Department of Science and Technology, India for the support through the Advanced Materials Research Unit.

[1] R. Ferrando, J. Jellinek, and R. L. Johnston, Chem. Rev. (Washington, D.C.) **108**, 845 (2008).

[2] J. Bansmann, S. H. Baker, C. Binns, J. A. Blackman, J.-P. Bucher, J. Dorantes-Davila, V. Dupuis, L. Favre, D. Kechrakos, A. Kleibert, K.-H. Meiwes-Broer, G. M. Pastor, A. Perez, O. Toulemonde, K. N. Trohidou, J. Tuaillon, and Y. Xie, Surf. Sci. Rep. **56**, 189 (2005).

[3] J. H. Sinfelt, *Bimetallic Catalysts: Discoveries, Concepts and*

Applications (Wiley, New York, 1983).
[4] N. Toshima and T. Yonezawa, New J. Chem. **22**, 1179 (1998).
[5] A. V. Ruban, H. L. Skriver, and J. K. Norskov, Phys. Rev. B **59**, 15990 (1999).
[6] G. Bozzolo, J. Ferrante, R. D. Noebe, B. Good, F. S. Honecy, and P. Abel, Comput. Mater. Sci. **15**, 169 (1999).
[7] F. Besenbacher, I. Chorkendorff, B. S. Clausen, B. Hammer, A. M. Molenbroek, J. K. Norskov, and I. Stensgaard, Science **279**, 1913 (1998).
[8] A. M. Molenbroek, S. Haukka, and B. S. Clausen, J. Phys. Chem. B **102**, 10680 (1998).
[9] A. Bongiorno and U. Landman, Phys. Rev. Lett. **95**, 106102 (2005).
[10] E. Kaxiras, Phys. Rev. Lett. **64**, 551 (1990).
[11] G. H. Guvelioglu, P. Ma, X. He, R. C. Forrey, and H. Cheng, Phys. Rev. Lett. **94**, 026103 (2005); Yang Jinlong, Xiao Chuanyun, Xia Shangda, and Wang Kelin, Phys. Rev. B **48**, 12155 (1993); R. Q. Zhang, T. S. Chu, H. F. Cheung, N. Wang, and S. T. Lee, *ibid.* **64**, 113304 (2001); J. Gavnholt and J. Schiøtz, *ibid.* **77**, 035404 (2008); D. R. Alfonso, S.-Y. Wu, C. S. Jayanthi, and E. Kaxiras, *ibid.* **59**, 7745 (1999); S. K. Nayak, S. E. Weber, P. Jena, K. Wildberger, R. Zeller, P. H. Dederichs, V. S. Stepanyuk, and W. Hergert, *ibid.* **56**, 8849 (1997); H. Kawamura, V. Kumar, and Y. Kawazoe, *ibid.* **70**, 193402 (2004).
[12] L. Holmgren, H. Gronbeck, M. Andersson, and A. Rosen, Phys. Rev. B **53**, 16644 (1996).
[13] S. Nonose, Y. Sone, K. Onodera, S. Sudo, and K. Kaya, J. Phys. Chem. **94**, 2744 (1990).
[14] G. C. Bond, *Heterogeneous Catalysis*, 2nd ed. (Clarendon Press, Oxford, 1987).
[15] A. Nakajima, T. Kishi, T. Sugioka, Y. Sone, and K. Kaya, J. Phys. Chem. **95**, 6833 (1991).
[16] A. Pramann, K. Koyasu, and A. Nakajima, J. Phys. Chem. A **106**, 2483 (2002).
[17] R. L. Whetten, D. M. Cox, D. J. Trevor, and A. Kaldor, Phys. Rev. Lett. **54**, 1494 (1985).
[18] K. Hoshino, T. Naganuma, K. Watanabe, Y. Konishi, A. Nakajima, and K. Kaya, Chem. Phys. Lett. **239**, 369 (1995).
[19] Vienna *ab initio* Simulation Package (VASP), Technische Universität Wien, 1999; G. Kresse and J. Hafner, Phys. Rev. B **47**, 558 (1993); G. Kresse and J. Furthmuller, *ibid.* **54**, 11169 (1996).
[20] P. E. Blöchl, Phys. Rev. B **50**, 17953 (1994).
[21] G. Kresse and D. Joubert, Phys. Rev. B **59**, 1758 (1999).
[22] J. P. Perdew, K. Burke, and M. Ernzerhof, Phys. Rev. Lett. **77**, 3865 (1996).
[23] M. C. Payne, M. P. Teter, D. C. Allan, T. A. Arias, and J. D. Joannopoulos, Rev. Mod. Phys. **64**, 1045 (1992).
[24] S. Datta, M. Kabir, S. Ganguly, B. Sanyal, T. Saha-Dasgupta, and A. Mookerjee, Phys. Rev. B **76**, 014429 (2007).
[25] *Theory of Atomic and Molecular Clusters*, edited by J. Jellinek (Springer, Berlin, 1999), p. 277, and references therein.
[26] J. Jellinek and E. B. Krissinel, Chem. Phys. Lett. **258**, 283 (1996); E. B. Krissinel and J. Jellinek, *ibid.* **272**, 301 (1997).
[27] J. A. Alonso, Chem. Rev. (Washington, D.C.) **100**, 637 (2000).
[28] Mukul Kabir, D. G. Kanhere, and Abhijit Mookerjee, Phys. Rev. B **73**, 224439 (2006); T. M. Briere, M. H. F. Sluiter, V. Kumar, and Y. Kawazoe, *ibid.* **66**, 064412 (2002).
[29] O. Dieguez, M. M. G. Alemany, C. Rey, P. Ordejon, and L. J. Gallego, Phys. Rev. B **63**, 205407 (2001).
[30] E. K. Parks, L. Zhu, J. Ho, and S. J. Riley, J. Chem. Phys. **102**, 7377 (1995); N. N. Lathiotakis, A. N. Andriotis, M. Menon, and J. Connolly, *ibid.* **104**, 992 (1996).
[31] S. Datta, M. Kabir, T. Saha-Dasgupta, and A. Mookerjee (unpublished).
[32] S. Datta, Ph.D. thesis, S. N. Bose National Centre for Basic Sciences, 2008.
[33] X. Xu, S. Yin, R. Moro, and W. A. de Heer, Phys. Rev. Lett. **95**, 237209 (2005).
[34] S. Ganguly, M. Kabir, S. Datta, B. Sanyal, and A. Mookerjee, Phys. Rev. B **78**, 014402 (2008).
[35] A. Kant and B. Strauss, J. Chem. Phys. **41**, 3806 (1964).
[36] S. P. Walch, C. W. Bauschlicher, Jr., B. O. Roos, and C. J. Nelin, Chem. Phys. Lett. **103**, 175 (1983).
[37] C.-X. Su, D. A. Hales, and P. B. Amentrout, J. Chem. Phys. **99**, 6613 (1993).
[38] M. El-Batanouny, M. Strongin, G. P. Williams, and J. Colbert, Phys. Rev. Lett. **46**, 269 (1981).
[39] M. W. Ruckman and M. Strongin, Phys. Rev. B **29**, 7105 (1984); D. Prigge, W. Schlerk, and E. Bauer, Surf. Sci. Lett. **123**, L698 (1982).
[40] G. Kresse and J. Hafner, Surf. Sci. **459**, 287 (2000).
[41] K. P. Huber and G. Hertzberg, *Molecular Structure and Molecular Spectra IV: Constants of Diatomic Molecules* (Van Nostrand Reinhold, New York, 1979).
[42] N. Fujima and T. Yamaguchi, J. Phys. Soc. Jpn. **61**, 1724 (1992).